RSC Advances

PAPER

View Article Online
View Journal | View Issue

CrossMark click for updates

Cite this: *RSC Adv.*, 2015, **5**, 65949

The influence of polar (0001) zinc oxide (ZnO) on the structure and morphology of vanadyl phthalocyanine (VOPc)†

Alexandra J. Ramadan,*[a] Luke A. Rochford,[b] Mary P. Ryan,[a] Tim S. Jones[b] and Sandrine Heutz*[a]

Received 28th May 2015
Accepted 29th July 2015

DOI: 10.1039/c5ra10131j

www.rsc.org/advances

Metal oxide thin films are increasingly utilized in small molecular organic photovoltaic devices to facilitate electron transport and injection. Despite this there is little understanding of the influence these layers have on the structure of adjacent organic semiconductor layers. Here we use both O- and Zn-terminated (0001) single crystal zinc oxide (ZnO) as a model system to investigate the effect of a metal oxide surface on the growth of a molecular semiconductor, vanadyl phthalocyanine (VOPc). The surface reconstructions of these model surfaces are determined and the properties of thin films of VOPc deposited atop are investigated. The nature of the bulk truncation of the surface is found to have pronounced effects on both the morphology and crystal structure of these molecular films. This work highlights the importance of considering the effects of the chemical composition and surface termination of metal oxide films on the structure of adjacent molecular semiconductor films.

Open Access Article. Published on 29 July 2015. Downloaded on 8/17/2024 12:28:28 PM.
This article is licensed under a Creative Commons Attribution 3.0 Unported Licence.

Introduction

Metal oxide thin films are of increasing interest in organic electronic applications, driven primarily by the increase in efficiency observed in organic electronic devices upon their insertion between active layers and electrodes.[1] Of particular significance is zinc oxide (ZnO), the low work function and high electron mobility of which facilitates its use as an electron transporting layer in small molecule OPV devices.[2,3] Although there has been considerable work investigating the effects of a ZnO electron transporting layer on device performance little attention has been paid to its influence on the structure and morphology of the adjacent molecular semiconductor film.[4–6]

ZnO, in its hexagonal form, adopts a wurtzite crystal structure comprised of alternating layers of oxygen and zinc atoms along the *c*-axis of the unit cell. The (0001) surface (orthogonal to the *c*-axis) can be either O- or Zn-terminated (as a bulk truncation) and is often considered to be polar as a result of its singly terminated surface.[7,8] The workfunction of the surfaces is also affected, and is systematically higher in the O-terminated case compared to Zn-terminated for identical preparation methods.[9–11] In contrast the mixed termination surfaces of ZnO are considered to be non-polar due to the presence of both Zn- and O-atoms in the surface plane. In this work single crystals oriented to the (0001) Miller plane were used as model surfaces to prepare metallo-phthalocyanine (MPc) thin films. The MPc family of molecules have been widely used in small molecule OPVs and demonstrated to be compatible with ZnO interlayers. Studies on the behaviour of MPc molecules on ZnO single crystal surfaces have so far only focused on the planar MPcs; the behaviour of zinc phthalocyanine has been investigated theoretically and copper phthalocyanine experimentally on $(1\bar{1}00)$ oriented ZnO.[12–14] Surface chemistry and symmetry has been shown to affect the structure and morphology of thin films of MPc molecules. Much of the research in this area has been carried out on single crystal coinage metal surfaces while binary metal oxides represent a much smaller part of the literature.[15–18] The behaviour of non-planar MPc molecules, in particular vanadyl phthalocyanine (VOPc), on ZnO surfaces has to our knowledge not previously been investigated. VOPc has a permanent electric dipole moment, a feature which is not present in any of the planar MPc molecules. There is an obvious potential for interaction between the molecular dipole moment and the polar oxide surface, an interaction which makes this system interesting from a fundamental point of view.

Results and discussion

To prepare atomically flat surfaces of (0001) ZnO which were stable both in ambient atmospheres and UHV, single crystals of both O and Zn terminations were annealed in air at 927 °C for

[a]*Department of Materials, Imperial College London, Exhibition Road, London, SW7 2AZ, UK. E-mail: ar707@ic.ac.uk; s.heutz@ic.ac.uk*

[b]*Department of Chemistry, University of Warwick, Gibbet Hill Road, Coventry, CV4 7AL, UK*

† Electronic supplementary information (ESI) available: AFM images of ZnO surfaces with line profiles showing atomically high steps. Schematic showing the two reconstructions which make up the Zn-terminated surface. See DOI: 10.1039/c5ra10131j

Open Access Article. Published on 29 July 2015. Downloaded on 8/17/2024 12:28:28 PM.
This article is licensed under a Creative Commons Attribution 3.0 Unported Licence.

1 hour. Once cooled the crystals were loaded into the UHV chamber and low energy electron diffraction (LEED) measurements were carried out. O-terminated (0001) ZnO surfaces (Fig. 1) showed sharp $(\sqrt{3} \times \sqrt{3})R30°$ diffraction patterns with a low elastic background indicating that the surface had reconstructed, in contrast to reports by Götzen and co-workers. In their work, (1×1) LEED patterns were observed for surfaces prepared similarly, suggesting no surface reconstruction.[19] To ensure that this reconstruction was stable in both air and UHV the crystal was transferred back into ambient atmosphere and left in a clean sample box overnight. After this the sample was transferred into UHV once more and the LEED measurements were repeated, resulting in identical patterns. Annealing experiments performed in UHV to surface temperatures of 600 °C (well above the temperature used for VOPc growth) for 1 hour left the LEED pattern unchanged at elevated temperatures and on cooling to ambient. The surface topography was imaged using atomic force microscopy (AFM) (Fig. 1) in ambient air. The surface of the reconstructed O-terminated (0001) ZnO exhibited a roughness (R_q) of 301.4 pm and is comprised of stepped terraces approximately 400 pm high, (Fig. S1†). LEED patterns taken from identically prepared Zn-terminated (0001) surfaces showed that the Zn-terminated surface, like the O-terminated surface, had undergone a reconstruction (Fig. 1). However unlike the O-termination the Zn-terminated surface appears to be made up of two reconstructions: $(\sqrt{3} \times \sqrt{3})R30°$ and (2×2), highlighted by the difference in two-dimensional spot profiles in each pattern (Fig. S2†). This is also different from the previously reported structure which showed a pattern comprised of $(\sqrt{3} \times \sqrt{3})R30°$ and (6×6) reconstructions.[19] The AFM topography image of the surface (Fig. 1) shows a similar morphology to the O-terminated surface comprised of stepped terraces approximately 380 pm high (Fig. S3†). The surface is similarly rough, (R_q = 249.9 pm), and it would appear that the different chemical terminations of the surfaces are responsible for their reconstructions.

Growth of VOPc was carried out onto the O-terminated ZnO surfaces, held at an elevated substrate temperature (T_{sub} = 155 °C), to produce films with nominal thicknesses of 5, 10 and 30 nm (Fig. 2). At 5 nm thickness, VOPc films (R_q = 8.9 nm) were comprised of rectangular islands, the shape of which is conserved in 10 nm and 30 nm films. These islands adopt a higher aspect ratio as film thickness is increased and significant growth along the surface normal is observed, consequently there is an increase in roughness (R_q = 20.5 nm and 35.1 nm respectively). In all films the islands are present with a variety of sizes and heights and appear to be ripening during growth suggesting that growth is occurring *via* a Volmer–Weber (island) growth mode.[20]

In comparison, VOPc films grown on the Zn-terminated surface exhibit a subtle change in the morphology of the grains relative to those grown on the O-terminated surface (Fig. 3). The 5, 10 and 30 nm VOPc films on this Zn-terminated surface all possess a slightly higher roughness (R_q = 13.8, 21.9 and 45.5 nm respectively) than their O-terminated equivalents. This difference in morphology between the films on the O- and Zn-terminated surfaces becomes most pronounced at higher thicknesses (Fig. 4). At 50 nm thickness, VOPc on O-terminated ZnO is comprised of grains with complex morphology seemingly composed of rectangular building blocks (R_q = 52.7 nm). The equivalent film on the Zn-terminated surface exhibits less bare surface and the grains of VOPc demonstrate a needle-like morphology (R_q = 49.6 nm).

Despite both surfaces being prepared from single-crystalline ZnO and sharing the same symmetry as bulk truncations, there is clearly a difference in their interaction with VOPc molecules. This morphological change is concomitant with a change in the out-of-plane crystal structure of the VOPc films. X-ray diffraction experiments on the thinner films (5, 10 and 30 nm) proved unsuccessful due to the small number of strongly scattering atoms per unit cell, so only films with 50 nm thickness were used. XRD patterns from the VOPc/O-terminated ZnO showed three peaks corresponding to the VOPc layer (2θ = 12.9°, 26.2° and 28.6°). These peaks, indexed using the VOPc single crystal structure (CCDC no. 1017243), correspond to the $(01\bar{1})$, $(1\bar{3}\bar{2})$

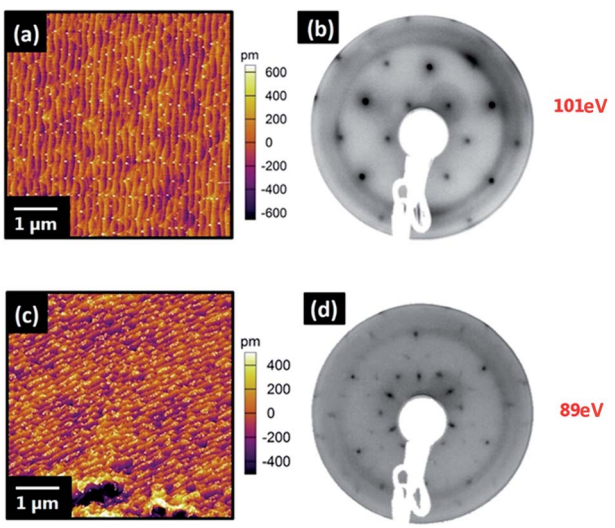

Fig. 1 (a) AFM topography image and (b) LEED pattern, captured at 101 eV, of oxygen terminated (0001) ZnO and (c) AFM topography image and (d) LEED pattern, captured at 89 eV, of zinc terminated (0001) ZnO.

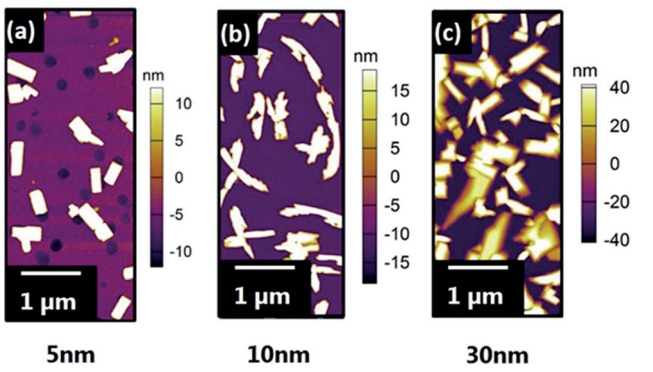

Fig. 2 AFM topography images of (a) 5 nm VOPc (b) 10 nm VOPc and (c) 30 nm VOPc on O-terminated (0001) ZnO reconstruction.

This journal is © The Royal Society of Chemistry 2015

Open Access Article. Published on 29 July 2015. Downloaded on 8/17/2024 12:28:28 PM.
This article is licensed under a Creative Commons Attribution 3.0 Unported Licence.

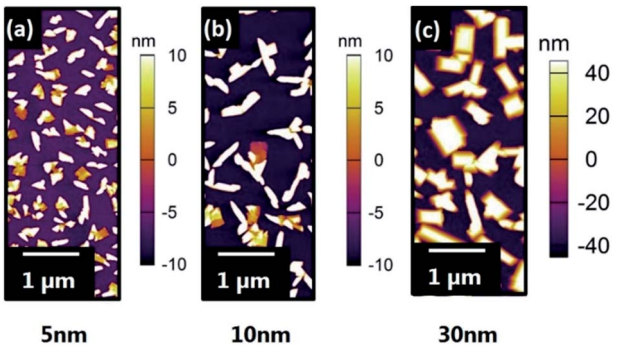

Fig. 3 AFM topography images of (a) 5 nm VOPc (b) 10 nm VOPc and (c) 30 nm VOPc on Zn-terminated (0001) ZnO reconstruction.

and $(22\bar{1})$ planes respectively. Diffractograms of the VOPc/Zn-terminated ZnO showed five peaks corresponding to the VOPc layer (2θ = 7.6°, 12.6°, 25.2°, 26.2° and 28.6°) which can be indexed as the (001), (110), (220), $(1\bar{3}\bar{2})$ and $(22\bar{1})$ planes respectively.

On both O- and Zn-terminated ZnO surfaces $(1\bar{3}\bar{2})$ and $(22\bar{1})$ VOPc peaks were observed, with additional (001) and (110) VOPc peaks present only for films grown on the Zn-surface. The difference in VOPc film structure and morphology between the ZnO substrates is evident. The prepared surfaces of the Zn and O faces have reconstructed differently, and the underlying cause of each reconstruction is the surface chemistry. Whilst the resolution limit in the AFM analysis precludes the direct determination of the atomic structure of each reconstruction, differences in the LEED data and effect on VOPc growth are clear. The common $(\sqrt{3} \times \sqrt{3})R30°$ reconstruction on the Zn- and O-surfaces may be the cause of the two shared VOPc orientations. Although the symmetry of this reconstruction is known from LEED patterns, the identity and binding site of the atoms comprising the reconstruction are not. Each surface could, in fact, show symmetrically similar but oppositely terminated (Zn or O) reconstructions. The termination of the surface also influences the work function, and the higher electron affinity of O–ZnO might contribute towards restricting the number of orientations adopted by the VOPc film.[11] Despite this ambiguity, the underlying cause of the difference in reconstruction between the surfaces (and the difference in VOPc film growth) is clearly the selected bulk truncation of the unit cell.

Incidentally XRD patterns from VOPc on O-terminated ZnO are identical to those observed in VOPc on polycrystalline (111) oriented copper iodide (CuI).[21] The use of single crystal CuI results in a single VOPc diffraction peak, $(1\bar{3}\bar{2})$, suggesting that grain boundaries and other associated features of polycrystalline films are the cause of the other two.[22,23] Therefore, although polycrystalline CuI thin films are significantly different from the ZnO single crystals used in terms of surface chemistry, morphology and crystal structure (cubic zinc-blende *vs.* hexagonal wurtzite respectively) there must be some similarities in their interactions with VOPc.

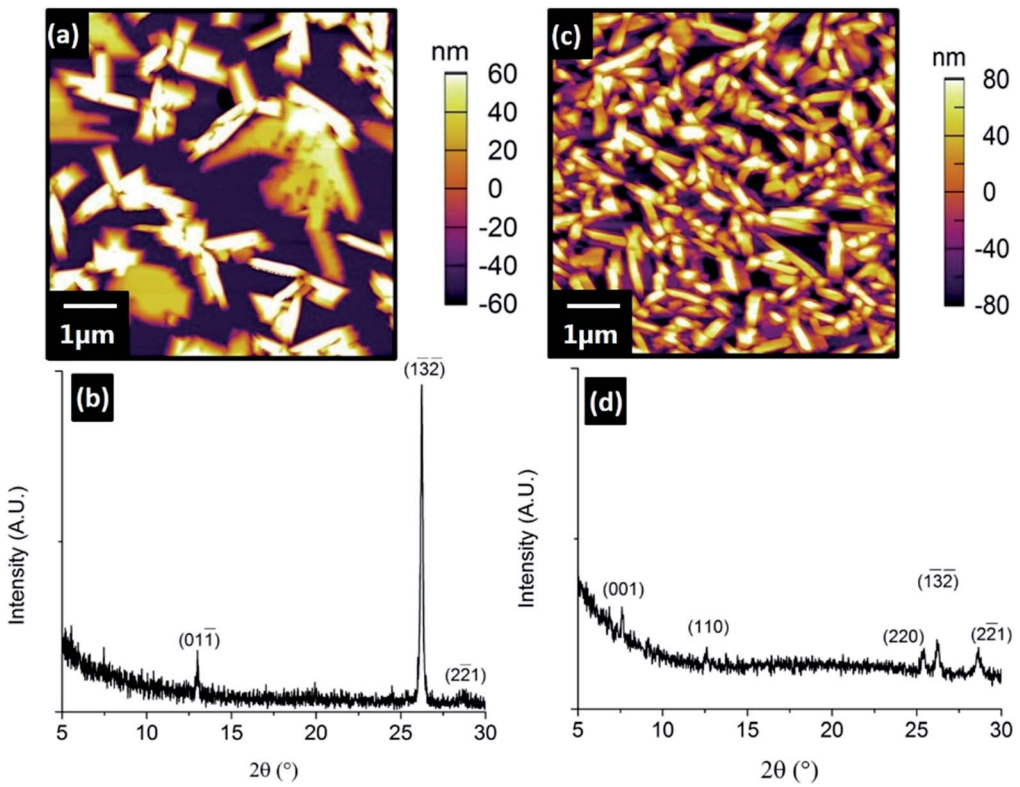

Fig. 4 (a) AFM topography image and (b) XRD pattern of 50 nm VOPc on O-terminated (0001) ZnO reconstruction (c) AFM topography image and (d) XRD pattern of 50 nm VOPc on Zn-terminated (0001) ZnO reconstruction.

Open Access Article. Published on 29 July 2015. Downloaded on 8/17/2024 12:28:28 PM.
This article is licensed under a Creative Commons Attribution 3.0 Unported Licence.

In either case the underlying cause of both the difference in reconstruction and the difference in VOPc film growth is clearly the chemistry of the ZnO surface.

Experimental

Zn- and O-terminated (0001) ZnO single crystals (10 × 10 mm, Pi-Kem, UK) were annealed in air using a Nabtherm (GmbH) LE/1/11/r6 box furnace. The crystals were heated using a modified version of the process previously reported by Götzen and co-workers,[19] at a rate of 50 °C min^{-1} to 927 °C where they were held for 60 min, then cooled at a rate of 25 °C min^{-1}. Crystals were loaded into a custom UHV multi-chamber system and LEED measurements were carried out. The crystals were then heated to 600 °C in UHV for 1 h and no change in LEED patterns was observed. VOPc (Acros Organics, BE) was triply purified by thermal gradient sublimation[24] and the resulting crystals were used for growth from a UHV evaporation cell (Karl Eberl GmbH) at 370 °C at a rate of 0.3 Å s^{-1}. Films of VOPc were grown at an elevated substrate temperature (T_{sub} = 155 °C) in the UHV system with a base pressure lower than 3 × 10^{-10} mbar. The substrate temperature was monitored using a K-type thermocouple mounted close to the sample and calibrated using an optical pyrometer. LEED patterns were collected with a SPECTALEED (Omicron®) rear-view MCP-LEED with nano-amp primary beam current. The images of these patterns were recorded using a digital CCD camera interfaced to a personal computer. AFM images were recorded using a MFP-3D AFM (Oxford Instruments Asylum Research, Santa Barbara, USA) in AC mode (tapping mode) using Olympus AC240-TS silicon tips. Thin film XRD patterns were obtained using a Panalytical X'Pert Pro MRD diffractometer with monochromatic Cu $K\alpha_1$ radiation.

Conclusions

The surface reconstructions of O- and Zn-terminated (0001) ZnO, after annealing in air, were determined and their effect on the structure and morphology of VOPc thin films has been observed. The reconstructed O-terminated surface resulted in VOPc thin films adopting an identical structure to the corresponding thin film on thin film (111) CuI. The VOPc film on reconstructed Zn-surfaces possesses some structural similarities but is markedly different from that on the O-terminated surface, highlighting the importance of the chemistry of the surface. This change in structure as a result of chemical termination suggests that the surface of metal oxide interlayers should be carefully considered when they are utilised in small molecule OPVs.

Acknowledgements

AJR and SH acknowledge support from the Engineering and Physical Sciences Research Council (EPSRC), UK (Grant no. EP/G037515/1). MPR thanks the EPSRC for the award of Grant no. EP/J500161/1. LAR and TSJ acknowledge support from the EPSRC, UK (Grant no. EP/H021388/1).

References

1 M. T. Greiner, M. G. Helander, W. M. Tang, Z. B. Wang, J. Qiu and Z. H. Lu, *Nat. Mater.*, 2011, **11**, 76–81.
2 S. Schumann, R. Da Campo, B. Illy, A. C. Cruickshank, M. A. McLachlan, M. P. Ryan, D. J. Riley, D. W. McComb and T. S. Jones, *J. Mater. Chem.*, 2011, **21**, 2381–2386.
3 J. Huang, Z. Yin and Q. Zheng, *Energy Environ. Sci.*, 2011, **4**, 3861.
4 B. A. MacLeod, B. J. Tremolet de Villers, P. Schulz, P. F. Ndione, H. Kim, A. J. Giordano, K. Zhu, S. R. Marder, S. Graham, J. J. Berry, A. Kahn and D. C. Olson, *Energy Environ. Sci.*, 2015, **8**, 592–601.
5 S. R. Cowan, P. Schulz, A. J. Giordano, A. Garcia, B. A. MacLeod, S. R. Marder, A. Kahn, D. S. Ginley, E. L. Ratcliff and D. C. Olson, *Adv. Funct. Mater.*, 2014, **24**, 4671–4680.
6 E. New, I. Hancox, L. A. Rochford, M. Walker, C. A. Dearden, C. F. McConville and T. S. Jones, *J. Mater. Chem. A*, 2014, **2**, 19201–19207.
7 S. Akhter, K. Lui and H. Kung, *J. Phys. Chem.*, 1985, **89**, 1958–1964.
8 G. Heiland and P. Kunstmann, *Surf. Sci.*, 1969, **13**, 72–84.
9 H. Moormann, D. Kohl and G. Heiland, *Surf. Sci.*, 1979, **80**, 261–264.
10 H. Moormann, D. Kohl and G. Heiland, *Surf. Sci. Lett.*, 1980, **100**, A393–A394.
11 R. Schlesinger, Y. Xu, O. T. Hofmann, S. Winkler, J. Frisch, J. Niederhausen, A. Vollmer, S. Blumstengel, F. Henneberger, P. Rinke, M. Scheffler and N. Koch, *Phys. Rev. B - Condens. Matter Mater. Phys.*, 2013, **87**, 1–5.
12 A. C. Cruickshank, C. J. Dotzler, S. Din, S. Heutz, M. F. Toney and M. P. Ryan, *J. Am. Chem. Soc.*, 2012, **134**, 14302–14305.
13 G. Mattioli, C. Melis, G. Malloci, F. Filippone, P. Alippi, P. Giannozzi, A. Mattoni and A. Amore Bonapasta, *J. Phys. Chem. C*, 2012, **116**, 15439–15448.
14 G. Mattioli, F. Filippone, P. Alippi, P. Giannozzi and A. A. Bonapasta, *J. Mater. Chem.*, 2012, **22**, 440–446.
15 Y. Wei, S. W. Robey and J. E. Reutt-Robey, *J. Phys. Chem. C*, 2008, **112**, 18537–18542.
16 N. Tsukahara, K. Noto, M. Ohara, S. Shiraki, N. Takagi, S. Shin and M. Kawai, *Phys. Rev. Lett.*, 2009, **102**, 167203.
17 M. Toader, P. Shukrynau, M. Knupfer, D. R. T. Zahn and M. Hietschold, *Langmuir*, 2012, **28**, 13325–13330.
18 L. A. Rochford, I. Hancox and T. S. Jones, *Surf. Sci.*, 2014, **628**, 62–65.
19 J. Götzen and G. Witte, *Appl. Surf. Sci.*, 2012, **258**, 10144–10147.
20 S. R. Forrest, *Chem. Rev.*, 1997, **97**, 1793–1896.
21 A. J. Ramadan, L. A. Rochford, D. S. Keeble, P. Sullivan, M. P. Ryan, T. S. Jones and S. Heutz, *J. Mater. Chem. C*, 2015, **3**, 461–465.
22 L. A. Rochford, A. J. Ramadan, S. Heutz and T. S. Jones, *Phys. Chem. Chem. Phys.*, 2014, **16**, 25404–25408.
23 L. A. Rochford, A. J. Ramadan, D. S. Keeble, M. P. Ryan, S. Heutz and T. S. Jones, *Adv. Mater. Interfaces*, 2015, **2**, 1–4.
24 A. R. McGhie, A. F. Garito and A. J. Heeger, *J. Cryst. Growth*, 1974, **22**, 295–297.

This journal is © The Royal Society of Chemistry 2015